



# HHS Public Access

## Author manuscript

*J Biomed Mater Res B Appl Biomater.* Author manuscript; available in PMC 2018 October 01.

Published in final edited form as:

*J Biomed Mater Res B Appl Biomater.* 2017 October ; 105(7): 2085–2092. doi:10.1002/jbm.b.33743.

## Tetracycline-incorporated polymer nanofibers as a potential dental implant surface modifier

**Marco C. Bottino<sup>1,2,3,\*</sup>, Eliseu A. Münchow<sup>1</sup>, Maria T. P. Albuquerque<sup>1</sup>, Krzysztof Kamocki<sup>1</sup>, Rana Shahi<sup>1</sup>, Richard L. Gregory<sup>1</sup>, Tien-Min G. Chu<sup>1</sup>, and Divya Pankajakshan<sup>1</sup>**

<sup>1</sup>Department of Biomedical & Applied Sciences, Division of Dental Biomaterials, Indiana University School of Dentistry (IUSD), Indianapolis, IN, 46202, USA

<sup>2</sup>Department of Biomedical Engineering, Indiana University Purdue University, Indianapolis, IN, 46202, USA

<sup>3</sup>Department of Anatomy & Cell Biology, Indiana University School of Medicine, Indianapolis, IN, 46202, USA

### Abstract

This study investigated the antimicrobial and osteogenic properties of titanium (Ti) disks superficially modified with tetracycline (TCH)-incorporated polymer nanofibers. The experiments were carried out in two phases. The first phase dealt with the synthesis and characterization (i.e., morphology, mechanical strength, drug release, antimicrobial activity, and cytocompatibility) of TCH-incorporated fibers. The second phase was dedicated to evaluating both the antimicrobial and murine-derived osteoprecursor cell (MC3T3-E1) response of Ti-modified with TCH-incorporated fibers. TCH was successfully incorporated into the submicron-sized and cytocompatible fibers. All TCH-incorporated mats presented significant antimicrobial activity against periodontal pathogens. The antimicrobial potential of the TCH-incorporated fibers-modified Ti was influenced by both the TCH concentration and bacteria tested. At days 5 and 7, a significant increase in MC3T3-E1 cell number was observed for TCH-incorporated nanofibers-modified Ti disks when compared to that of TCH-free nanofibers-modified Ti-disks and bare Ti. A significant increase in alkaline phosphatase (ALP) levels on the Ti disks modified with TCH-incorporated nanofiber on days 7 and 14 was seen, suggesting that the proposed surface promotes early osteogenic differentiation. Collectively, the data suggest that TCH-incorporated nanofibers could function as an antimicrobial surface modifier and osteogenic inducer for Ti dental implants.

### Keywords

electrospinning; nanofibers; titanium; osteoblasts; antimicrobial; tetracycline; coating

\*Correspondence to: Dr. Marco Cicero Bottino, Indiana University School of Dentistry, Department of Biomedical & Applied Sciences, Division of Dental Biomaterials, 1121 W. Michigan St. (DS270B), Indianapolis, IN, 46202, USA, Tel: +1-317-274-3725; fax: +1-317-278-7462. mbottino@iu.edu, (M.C. Bottino).

The authors received no financial support and declare no potential conflicts of interest with respect to authorship and/or publication of this article.

## INTRODUCTION

For over four decades, commercially pure titanium (cpTi) and titanium (Ti) alloys have been used for implant therapy due to their remarkable mechanical properties in load-bearing applications, low density, high corrosion resistance, and biocompatibility.<sup>1</sup> Of note, the basis for using Ti in implant dentistry is predicated on its ability to achieve a direct structural and functional interface with living bone (i.e., osseointegration), which has allowed for the successful restoration of masticatory function in partially and completely edentulous patients.<sup>2, 3</sup> Regrettably, despite accumulating evidence regarding the positive role played by implant surface modification both texture/microstructure and chemistry on bone integration<sup>4–7</sup>, the risk of infection (peri-implantitis), and thus early implant loss<sup>8, 9</sup>, still embodies a major clinical concern.

Peri-implantitis has been defined as a progressive and irreversible polymicrobial infection affecting soft and hard tissues around dental implants. It is well-established that subgingival anaerobic Gram-negative bacteria such as *Prevotella intermedia*, *Prevotella nigrescens*, *Aggregatibacter actinomycetemcomitans*, *Porphyromonas gingivalis*, *Treponema denticola*, and *Tannerella forsythia* bacteria associated with peri-implantitis are similar to those related to periodontal disease.<sup>8, 9</sup> Simply speaking, once peri-implantitis is established, one needs to focus on the decontamination of the implant surfaces, control of inflammation, and inhibition of progressive bone loss. Over the years, apart from the non-surgical and surgical approaches performed to manage the disease, alternative and/or complementary treatment strategies such as those involving laser and photodynamic therapies have been investigated.

Significant advances in nanotechnology have helped to pave the way toward the development of antimicrobial coatings that could be used to avoid implant infection.<sup>10–13</sup> Meanwhile, recent research highlighted the prospective anabolic effects associated with tetracycline-derivatives (e.g., doxycycline and minocycline) as their use seemed to enhance cell proliferation.<sup>14</sup> Nonetheless, and to the best of our knowledge, no single dental implant that conjugates bone promoting and antimicrobial surface properties derived from tetracycline-derivatives is available. In recent years, electrospinning has been deemed a facile approach to synthesize antibiotic-containing polymer nanofibers with significant antimicrobial properties<sup>15, 16</sup> and ability to prevent bacterial infection.<sup>17, 18</sup> Worth mentioning, electrospinning has demonstrated to be a potential method to modify the surface of titanium implants with nanofibers as a coating material, contributing to potentially minimize early implant loss, especially in those patients who are at high risk of periodontal disease.

The purpose of this study was to investigate the antimicrobial and osteogenic properties of titanium (Ti) dental implant disks superficially modified with tetracycline (TCH)-incorporated polymer nanofibers.

## MATERIALS AND METHODS

The experiments were carried out in two phases. The first phase dealt with the synthesis and characterization (i.e., morphology, mechanical strength, antimicrobial activity, and

cytocompatibility) of TCH-incorporated polymer fibers. The second phase was dedicated to evaluating both the antimicrobial and biological osteoprecursor cell response (i.e., proliferation and differentiation) of TCH-incorporated fibers-modified Ti.

## Phase I

**Reagents**—Poly(DL-lactide) (PLA, inherent viscosity: 0.55-0.75 dL/g in CHCl<sub>3</sub>) and poly( $\epsilon$ -caprolactone) (PCL, inherent viscosity: 1.29 dL/g in CHCl<sub>3</sub>) were purchased from Lactel Absorbable Polymers (Durect Corporation, Birmingham, AL, USA). Type-B Gelatin (GEL) from bovine skin (bloom no. 225), tetracycline hydrochloride (TCH, molecular weight [Mw] 480.90 g/mol), hexamethyldisilazane (HMDS), formaldehyde, and 1,1,1,3,3,3-hexafluoro-2-propanol (HFP) were acquired from Sigma-Aldrich (St. Louis, MO). Brain heart infusion (BHI) culture media containing 5 g/L yeast extract (BHI-YE) with 5% v/v Vitamin K/hemin solution were obtained from Difco Laboratories (Detroit, MI) and Thermo Scientific (Pittsburgh, PA), respectively. Phosphate-buffered saline, ethanol, and blood agar plates supplemented with 5% sheep blood were obtained from Thermo Fisher Scientific (Fair Lawn, NJ).

**Synthesis and characterization of TCH-incorporated polymer fibers**—A polymer solution was prepared by solubilizing PLA, PCL, and gelatin/GEL (ratio of 2:2:1, w/w) in HFP to obtain a 7.5 wt.% solution. Next, TCH was added to the polymer solution at different concentrations (5, 10, and 25 wt.%, relative to the total polymer weight) and stirred overnight. Then, each solution was individually loaded into a plastic syringe (Beckton-Dickson, Franklin Lakes, NJ, USA) fitted with a 27G metallic blunt-tip needle and spun into fibrous mats using the following electrospinning parameters: 1.0 mL·h<sup>-1</sup>, 18 cm distance, and 20-25 kV. To ensure complete elimination of any residual solvent, the processed fibrous mats were dried for 48 h under vacuum at room temperature (RT) and then stored at 4°C prior to use.<sup>15</sup>

The processed fibers were characterized by morphological, chemical, mechanical, drug release, antimicrobial, and cytotoxicity analyses following previously established protocols.<sup>15</sup> For the morphological analysis, samples were taken from each mat, mounted on Al stubs, sputter-coated with Au-Pd, and imaged using a scanning electron microscope (SEM, JSM-5310LV, JEOL, Tokyo, Japan). Fourier transform infrared (FTIR) spectroscopy in attenuated total reflection mode (ATR/FTIR-4100, JASCO, Easton, MD, USA) was used to evaluate the possibility of an interaction of chemical bonds between TCH and the polymers. For the mechanical analyses, samples were tested using tensile testing (expert 5601, ADMET, Norwood, MA, USA), under dry and hydrated (24 h in PBS) conditions.<sup>15</sup> For the drug release analysis, high-performance liquid chromatography (HPLC) was conducted. TCH-incorporated mats (15 × 15 mm<sup>2</sup>, n=4/group) were weighed and incubated in 10 mL of PBS at 37°C. 1 mL aliquots were collected at different time points. Equal amounts of fresh PBS were added back to the incubation media following aliquot retrieval. The TCH content (absorption peak 276.8 nm) was determined using HPLC equipped with a UV-Vis detector (Perkin-Elmer, Shelton, CT, USA). TCH solutions at known concentrations were used to obtain the calibration curves.<sup>15</sup>

**Antimicrobial properties of electrospun TCH-incorporated polymer fibers**—The antimicrobial activity of the fibrous mats was assessed against *Aggregatibacter actinomycetemcomitans* (*Aa*, ATCC 29522), *Fusobacterium nucleatum* (, ATCC 10953), *Porphyromonas gingivalis* (, ATTC 33277), and *Prevotella intermedia* (, ATCC 25611) using the agar diffusion assay. All bacteria were cultivated in Brain Heart Infusion (BHI) broth supplemented with 5 g yeast extract/L and 5% v/v vitamin K+ hemin (BHI-YE; Becton, Dickinson and Company) at 37°C in an anaerobic GasPak jar for 24 h. After that, 100 µL was pipetted onto blood agar plates, spread and placed in an incubator under anaerobic conditions. Subsequently, the fibrous mats ( $\phi = 5$  mm, n=3/group) were ultraviolet (UV)-irradiated for disinfection purposes and placed on cultured blood agar plates containing bacterial lawns of *Aa*, *Fn*, *Pg*, and *Pi*. After 5 days of incubation the inhibition zones were measured (in mm) using a transparent plastic ruler.<sup>15, 20</sup>

**Cytocompatibility of TCH-incorporated polymer fibers**—Mouse calvaria-derived osteoprecursor cells (MC3T3-E1, American Type Culture Collection, ATCC, CRL-2593, Manassas, VA, USA) were cultured in minimum essential medium (MEM, GIBCO/Invitrogen, Grand Island, NY, USA) supplemented with 10% fetal bovine serum (HyClone Laboratories Inc., South Logan, UT, USA), 1% L-glutamine (Hyclone), and 1% penicillin-streptomycin (Sigma) in a humidified incubator at 37°C, with 5% CO<sub>2</sub>.<sup>21</sup> Replacement of the culture medium was performed every other day. MC3T3-E1 cells at passages 15-17 were used. Cytotoxicity assays were performed according to the guidelines (10993-5) provided by the International Standards Organization.<sup>22</sup> Briefly, electrospun mats (15 × 15 mm<sup>2</sup>) were disinfected by UV irradiation (30 min/side) and then incubated in culture media (1 cm<sup>2</sup>/mL) for 48 h at 37°C. The extracts were filtered through a membrane (Millipore<sup>®</sup>) and serially diluted (100, 50, 25, 12.5 and 6.25%). A 0.3% phenol solution was assayed to serve as the positive control. MC3T3-E1 cells were seeded on 96-well plates at a density of 3000 cells/mL, and were allowed to attach. After 4 h, the media was replaced by the distinct extract dilutions obtained from the electrospun mats, negative, and positive controls. 100 µL of each extract was dispensed into each well. Control columns of four wells were prepared with a medium without cells (blank), and a medium with cells but without the extract (100% survival). The microplate was then incubated under 5% CO<sub>2</sub> humidified atmosphere. After 72 h, 20 µL of CellTiter 96 AQueous One Solution Reagent (Promega, Madison, WI, USA) was added to the test wells and allowed to react for 2 h (37°C and 5% CO<sub>2</sub>). Incorporated dye was measured by reading the absorbance at 490 nm in a microplate reader against a blank column.<sup>15</sup> Results are shown as the mean value (±SD) of the mean.

## Phase II

**TCH-incorporated fiber-modified Ti - antimicrobial and cell-related studies**—Commercially pure Ti disks (12-mm diameter and 1-mm thick) were procured from United Titanium, Inc. (Wooster, OH, USA), cleaned overnight by sonication with deionized water, dried in air, mounted on a stainless steel aluminum foil-covered mandrel, and modified by TCH-incorporated fibers using the aforementioned electrospinning parameters for ca. 8 min. The antimicrobial activity of the TCH-incorporated fiber-modified Ti (n=3/group) was evaluated against *Aa*, *Fn*, *Pg*, and *Pi* using the agar diffusion protocol, as previously described.

Cell proliferation ( $n=4$ /group) was assessed using the WST-1<sup>®</sup> (Roche Diagnostics Corporation, Indianapolis, IN, USA) assay after 1, 3, 5, and 7 days. All samples were UV-sterilized before cell seeding. In brief,  $1\times10^4$  cells at passage 15 were seeded on each of the Ti disks in 24-well culture plates. The media was changed every other day. On the day of analysis, 30  $\mu\text{L}$  of the assay reagent was added to 300  $\mu\text{L}$  of media in each well and allowed to react for 3 h at 37°C and 5% CO<sub>2</sub>. The incorporated dye was then measured by reading the absorbance at 450 nm in a microplate reader against the blank. Additional samples ( $N=2$ ) were included to qualitatively evaluate the morphology of the cells via SEM. Following samples' removal from the culture medium, they were fixed in buffered 4% formaldehyde (Sigma) and washed with PBS to remove unbound cells. Next, the samples were dehydrated using ethanol gradients, soaked in ethanol/hexamethyldisilazane (HMDS) gradients, and then incubated in 100% HMDS.<sup>15</sup> Upon air-drying; the samples were mounted on Al stubs and sputter-coated with Au-Pd prior to imaging.

MC3T3-E1 cells osteogenic differentiation on the TCH-incorporated nanofiber-modified Ti disks was quantitatively determined by alkaline phosphatase (ALP) activity at days 1, 3, 7, and 14 using an ALP assay kit (SensoLyte pNPP, AnaSpec, Fremont, CA, USA). The assay is based on the conversion of *p*-nitrophenyl phosphate (pNPP) to *p*-nitrophenol by the enzyme. Briefly, the cells were seeded on the nanofiber-modified Ti disks ( $n=4$ ) at a density of  $3\times10^6$  and cultured in osteogenic differentiation media (Lonza, Walkersville, MD, USA) for 14 days. On specific days, the cells were digested using lysis buffer (200  $\mu\text{L}$ ) and subjected to freeze-thaw cycles. The cell suspension was centrifuged for 10 min at 4°C. 50  $\mu\text{L}$  of the supernatant was added to each well of a 96-well plate and allowed to react for 15 min with the pNPP substrate solution (50  $\mu\text{L}$ ) at 37°C. Standards of 0–300 ng/mL *p*-nitrophenol were run in parallel. The absorbance of standards and samples were read at 405 nm. Protein concentrations of the sample supernatants were determined using a Pierce<sup>TM</sup> assay kit (Thermo Scientific, Waltham, MA, USA).

## STATISTICAL ANALYSIS

Data were statistically analyzed (SigmaPlot, version 12, Systat Software, Inc., San Jose, CA, USA) using One-Way (for fiber diameter, cytotoxicity, and antimicrobial [of nanofiber-modified Ti disks] data) or Two-Way (for mechanical, antimicrobial [of nanofibers], and cell proliferation data) Analysis of Variance and Tukey's test for multiple comparisons. A 5% significance level was used for all analyses.

## RESULTS

### Phase I

According to Figure 1A, all electrospun mats demonstrated a smooth and bead-free fibrous architecture regardless of the presence and concentration of TCH. The diameter of the fibers increased with TCH incorporation, although only at 25 wt.%, which resulted in a higher ( $p < 0.05$ ) diameter when compared to the other groups. With regard to the fiber diameter distribution, the TCH-free mat displayed the most homogeneous and narrow distribution (Figure 1B). Moreover, TCH was successfully incorporated (FTIR data, Figure 1C) into the

fibers, confirmed by the presence of characteristic peaks ( $1,615\text{ cm}^{-1}$  and  $1,581\text{ cm}^{-1}$ ) observed within the TCH powder and TCH-incorporated mats.

Results regarding mechanical performance of the mats are presented in Figure 2. There was a statistically significant ( $p < 0.001$ ) interaction between the factors “electrospun mat” and “storage condition,” except for tensile strength ( $p=0.981$ ). Overall, while the incorporation of a low (5 wt.%) TCH amount did not alter the mechanical properties, the addition of medium (10 wt.%) and high (25 wt.%) TCH contents seemed to improve the evaluated properties, particularly the Young’s modulus. The only exception was seen for the elongation at break, which, under dry conditions, was progressively reduced with increased TCH content ( $p < 0.05$ ).

As shown in Figure 3, TCH was mostly released within the first 24 h, with the more concentrated groups releasing a greater TCH amount—followed by a slow and continuous release up to 7 days. Based on the results shown in Figure 4A, all TCH-incorporated mats presented significant antimicrobial activity, producing even higher ( $p < 0.05$ ) inhibition zones than the control (chlorhexidine). Noteworthy, *Pg* and *Pi*, respectively, demonstrated the highest and the lowest susceptibility to TCH. The cell viability data (Figure 4B) indicated that all electrospun mats were considered biologically safe when compared to the phenol solution (positive control).

## Phase II

The antimicrobial potential of the TCH-incorporated nanofibers-modified Ti disks was influenced by both the TCH concentration and bacteria specie investigated (Figure 5). When tested against *Aa* and *Fn*, the greater the TCH concentration, the greater the antimicrobial activity ( $p < 0.05$ ); nevertheless, when tested against *Pg* and *Pi*, TCH concentrations beyond 10 wt.% did not enhance antimicrobial activity ( $p > 0.05$ ).

Results regarding cell proliferation are given in Figure 6A. A consistent increase in cell proliferation was seen from day 1 to day 7. At days 5 and 7, a significant increase in cell number was observed for TCH-incorporated nanofibers-modified Ti disks when compared to that of TCH-free nanofibers-modified Ti-disks and bare Ti. Meanwhile, ALP activity was similar for all groups at days 1 and 3 (Figure 6B). However, there was a significant increase in ALP levels of MC3T3-E1 cells on Ti disks modified with TCH-incorporated nanofibers (5, 10, and 25 wt.%) on days 7 and 14, suggesting that the proposed surface modification promotes early osteogenic differentiation when compared to both TCH-free and bare Ti groups. The ALP activity decreased by day 14 in all the samples, indicating the onset of the ECM mineralization phase (Figure 6B). There was no statistically significant difference in ALP levels among the TCH-incorporated fibers-modified Ti. Representative SEM images further demonstrated that all Ti-disks supported cell adhesion, spreading, and proliferation (Figure 7).

## DISCUSSION

The present research holds potential clinical relevance, since there is strong evidence concerning the failure rate of implants in periodontally-compromised individuals<sup>8, 9</sup>, clearly

stressing the need for an implant surface with antimicrobial characteristics to prevent and/or fight pathogens.

In this investigation, TCH-incorporated nanofibers were successfully synthesized via electrospinning. The presence of TCH did not negatively affect the architecture and morphology of the fibers (Figure 1A). Although a slight increase in fiber diameter occurred upon TCH incorporation (Figure 1B), especially for the most concentrated group (~ 64.3%), this increase seemed not to compromise the applicability of the fibers, since they were still homogeneous and within the submicron-sized range. Indeed, one could expect that the hydroxyl groups present in the molecular structure of TCH would increase the intermolecular interactions (e.g., hydrogen bonds) with the polymer, or the viscosity of the polymer solution, thus resulting in thicker fibers.

Regarding the mechanical performance of the fibrous mats, the tensile strength was not affected by the presence/concentration of TCH and storage conditions (Figure 2), and this may be a reason for the similar fiber morphology exhibited by all mats. Conversely, TCH concentration played a role in the other properties tested: while the Young's modulus improved with greater TCH content, the elongation at break was significantly reduced. It can be suggested that on one hand, the presence of TCH may produce strong fibers (i.e., high Young's modulus), probably due to the formation of intermolecular interactions or an enhanced crystallization effect; on the other hand, TCH may turn the fiber brittle, reducing its stretching ability. Nonetheless, it is worth mentioning that upon immersion into PBS, a significant increase in elongation at break and significant decrease in Young's modulus were observed, probably due to the burst release of TCH from the fibers (Figure 3). The increase in stretching ability under wet conditions would be of utmost importance for the applications of the obtained fibers as a coating, especially because dental implants are commonly screwed into the bone which may evoke bleeding (wet environment).

Gelatin, a natural polymer that can be obtained by denaturing collagen, has shown nearly identical composition and biological properties to that of collagen.<sup>23</sup> Recently, blends of GEL and synthetic polymers were spun into fibrous scaffolds as potential skin grafts. It was demonstrated that increasing the GEL content led to quicker fibers degradation.<sup>24</sup> Based on the aforementioned, we hypothesized that the addition of GEL to the highly hydrophobic polymer blend (PLA:PCL) would lead to an increased solubility and quicker degradation, which could ultimately translate into faster TCH release. It has been known that upon implantation, a competition exists between implant integration and bacterial adhesion to the biomaterial surface.<sup>25</sup> Notably, a 6 h post-implantation period has been deemed crucial to the long-term success of an implantable device. Collectively, the microbiological data (i.e., TCH-incorporated mats and TCH-incorporated fibers-modified Ti disks) demonstrated significant antimicrobial properties against peri-implantitis-related pathogens.

Our cell viability data revealed that the TCH amounts released by the electrospun mats were not cytotoxic. More importantly, since the levels of TCH used might have played both a direct and indirect role in cell viability, we evaluated the effects of the TCH-incorporated nanofiber-modified Ti disks on the proliferation and differentiation of osteoprecursor (MC3T3-E1) cells. As previously stated, an increased cell proliferation at day 7 on TCH-

incorporated nanofiber-modified Ti was seen when compared to the control (bare Ti). Previous work by Gomes et al.<sup>14</sup> evaluated the dose-dependency effects of tetracyclines on human bone marrow cells. It was found that continuous exposure to doxycycline (1 and 5 µg/mL) and minocycline (1-10 µg/mL) caused an evident induction of cell proliferation from the first week onward. However, higher concentrations of doxycycline and minocycline negatively impact cell growth. In our study, the amount of TCH released led to increased cell proliferation. Meanwhile, to test our second hypothesis, MC3T3-E1 differentiation was assessed by ALP activity, an early marker of osteoblastic cell differentiation, which is divided into three phases: proliferation, maturation, and ECM mineralization. The highest enzyme level is found during the maturation phase (the second stage) of differentiation. Although an increased ALP expression was seen during the maturation phase (Day 7) on TCH-incorporated fibers-modified Ti, it is worth stating here that conflicting results have been reported on the effect of tetracyclines (minocycline, doxycycline, and tetracycline hydrochloride) on osteogenic differentiation. Overall, the higher the dose, the greater the inhibition on preosteoblasts differentiation and bone-related protein expression (e.g., bone morphogenic protein-2).<sup>26</sup> In this way, recent research reported positive effects when using small doses of doxycycline (0.1 and 1.0 mM) on osteoprecursor cells differentiation at an early stage.<sup>27</sup> Furthermore, osteoinductive effects were also seen upon treatment, which was attributed to the upregulation of estrogen receptor (ER)-α. Here, the higher ALP levels on preosteoblasts cultured on TCH-incorporated nanofiber-modified Ti suggest that the proposed surface modification with TCH might enhance peri-implant bone formation upon implantation. Noteworthy, no visible signs of fiber peeling/detachment from the Ti disks were observed throughout the experiments. However, future studies should investigate the bonding ability between the TCH-incorporated fibers to titanium prior to its pre-clinical evaluation.

## CONCLUSION

Collectively, the data suggest that TCH-incorporated polymer nanofibers could function as an antimicrobial surface modifier and osteogenic inducer for titanium dental implants.

## Acknowledgments

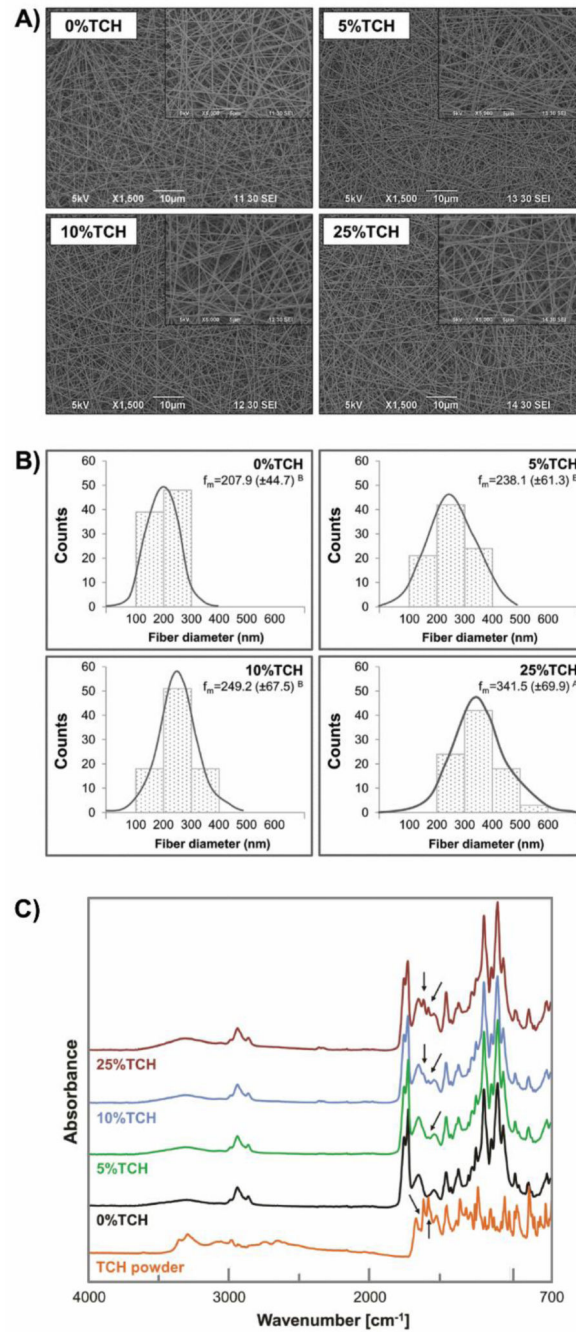
This research project was partially supported by a Delta Dental Foundation Grant. M.C.B. also acknowledges start-up funds from IUSD and funding from NIH/NIDCR (Grant#DE023552).

## References

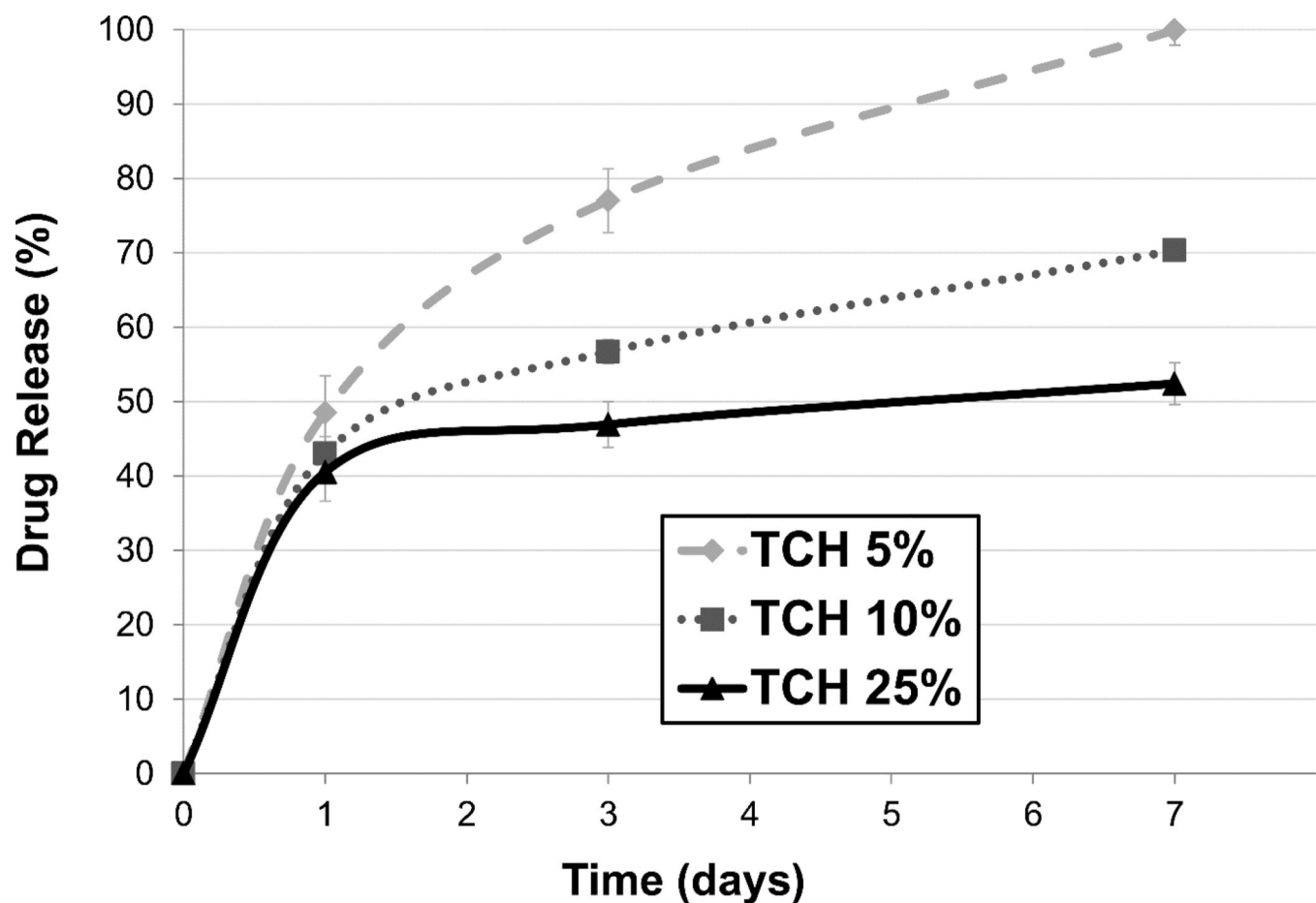
1. Adell R, Lekholm U, Rockler B, Branemark PI. A 15-year study of osseointegrated implants in the treatment of the edentulous jaw. *Int J Oral Surg.* 1981; 10:387–416. [PubMed: 6809663]
2. Bränemark PI, Adell R, Albrektsson T, Lekholm U, Lundkvist S, Rockler B. Osseointegrated titanium fixtures in the treatment of edentulousness. *Biomaterials.* 1983; 4:25–8. [PubMed: 6838955]
3. Adell R, Eriksson B, Lekholm U, Bränemark PI, Jemt T. Long-term follow-up study of osseointegrated implants in the treatment of totally edentulous jaws. *Int J Oral Maxillofac Implants.* 1990; 5:347–59. [PubMed: 2094653]
4. Shalabi MM, Gortemaker A, Van't Hof MA, Jansen JA, Creugers NH. Implant surface roughness and bone healing: a systematic review. *J Dent Res.* 2006; 85:496–500. [PubMed: 16723643]

5. Le Guéhennec L, Soueidan A, Layrolle P, Amouriq Y. Surface treatments of titanium dental implants for rapid osseointegration. *Dent Mater*. 2007; 23:844–54. [PubMed: 16904738]
6. Mendonça G, Mendonça DB, Simões LG, Araújo AL, Leite ER, Duarte WR, Aragão FJ, Cooper LF. The effects of implant surface nanoscale features on osteoblast-specific gene expression. *Biomaterials*. 2009; 30:4053–62. [PubMed: 19464052]
7. Coelho PG, Jimbo R, Tovar N, Bonfante EA. Osseointegration: hierarchical designing encompassing the macrometer, micrometer, and nanometer length scales. *Dent Mater*. 2015; 31:37–52. [PubMed: 25467952]
8. Monje A, Alcoforado G, Padial-Molina M, Suarez F, Lin GH, Wang HL. Generalized aggressive periodontitis as a risk factor for dental implant failure: a systematic review and meta-analysis. *J Periodontol*. 2014; 85:1398–407. [PubMed: 24835415]
9. Chrcanovic BR, Albrektsson T, Wennerberg A. Periodontally compromised vs. periodontally healthy patients and dental implants: a systematic review and meta-analysis. *J Dent*. 2014; 42:1509–27. [PubMed: 25283479]
10. Zhao L, Chu PK, Zhang Y, Wu Z. Antibacterial coatings on titanium implants. *J Biomed Mater Res B Appl Biomater*. 2009; 91:470–80. [PubMed: 19637369]
11. Puckett SD, Lee PP, Ciombor DM, Aaron RK, Webster TJ. Nanotextured titanium surfaces for enhancing skin growth on transcutaneous osseointegrated devices. *Acta Biomater*. 2010; 6:2352–62. [PubMed: 20005310]
12. Seil JT, Webster TJ. Antimicrobial applications of nanotechnology: methods and literature. *Int J Nanomedicine*. 2012; 7:2767–81. [PubMed: 22745541]
13. Zhang L, Yan J, Yin Z, Tang C, Guo Y, Li D, Wei B, Xu Y, Gu Q, Wang L. Electrospun vancomycin-loaded coating on titanium implants for the prevention of implant-associated infections. *Int J Nanomedicine*. 2014; 23:3027–36.
14. Gomes PS, Santos JD, Fernandes MH. Cell-induced response by tetracyclines on human bone marrow colonized hydroxyapatite and Bonelike. *Acta Biomater*. 2008; 4:630–7. [PubMed: 18291737]
15. Bottino MC, Kamocki K, Yassen GH, Platt JA, Vail MM, Ehrlich Y, Spolnik KJ, Gregory RL. Bioactive nanofibrous scaffolds for regenerative endodontics. *J Dent Res*. 2013; 92:963–9. [PubMed: 24056225]
16. Albuquerque MTP, Valera MC, Nakashima M, Nör JE, Bottino MC. Tissue-engineering-based strategies for regenerative endodontics. *J Dent Res*. 2014; 93:1222–31. [PubMed: 25201917]
17. Li LL, Wang LM, Xu Y, Lv LX. Preparation of gentamicin-loaded electrospun coating on titanium implants and a study of their properties in vitro. *Arch Orthop Trauma Surg*. 2012; 132:897–903. [PubMed: 22373914]
18. Gilchrist SE, Lange D, Letchford K, Bach H, Fazli L, Burt HM. Fusidic acid and rifampicin co-loaded PLGA nanofibers for the prevention of orthopedic implant associated infections. *J Control Release*. 2013; 170:64–73. [PubMed: 23639451]
19. Sapadin AN, Fleischmajer R. Tetracyclines: nonantibiotic properties and their clinical implications. *J Am Acad Dermatol*. 2006; 54:258–65. [PubMed: 16443056]
20. Palasuk J, Kamocki K, Hippenmeyer L, Platt JA, Spolnik KJ, Gregory RL, Bottino MC. Bimix antimicrobial scaffolds for regenerative endodontics. *J Endod*. 2014; 40:1879–84. [PubMed: 25201643]
21. Rowe MJ, Kamocki K, Pankajakshan D, Li D, Bruzzaniti A, Thomas V, Blanchard SB, Bottino MC. Dimensionally stable and bioactive membrane for guided bone regeneration: An in vitro study. *J Biomed Mater Res B Appl Biomater*. 2015 May 7. [Epub ahead of print].
22. International Organization for Standardization. ISO 10993-5:2009 ed. 2009. ISO 10993-5: biological evaluation of medical devices – Part 5: tests for in vitro cytotoxicity.
23. Zeugolis DI, Khew ST, Yew ES, Ekputra AK, Tong YW, Yung LY, Hutmacher DW, Sheppard C, Raghunath M. Electro-spinning of pure collagen nano-fibres - just an expensive way to make gelatin? *Biomaterials*. 2008; 29:2293–305. [PubMed: 18313748]
24. Jeong SI, Lee AY, Lee YM, Shin H. Electrospun gelatin/poly(L-lactide-co-epsilon-caprolactone) nanofibers for mechanically functional tissue-engineering scaffolds. *J Biomater Sci Polym Ed*. 2008; 19:339–57. [PubMed: 18325235]

25. Hetrick EM, Schoenfisch MH. Reducing implant-related infections: active release strategies. *Chem Soc Rev.* 2006; 35:780–9. [PubMed: 16936926]
26. Park JB. Effects of doxycycline, minocycline, and tetracycline on cell proliferation, differentiation, and protein expression in osteoprecursor cells. *J Craniofac Surg.* 2011; 22:1839–42. [PubMed: 21959447]
27. Park JB. Low dose of doxycycline promotes early differentiation of preosteoblasts by partially regulating the expression of estrogen receptors. *J Surg Res.* 2012; 178:737–42. [PubMed: 22541278]

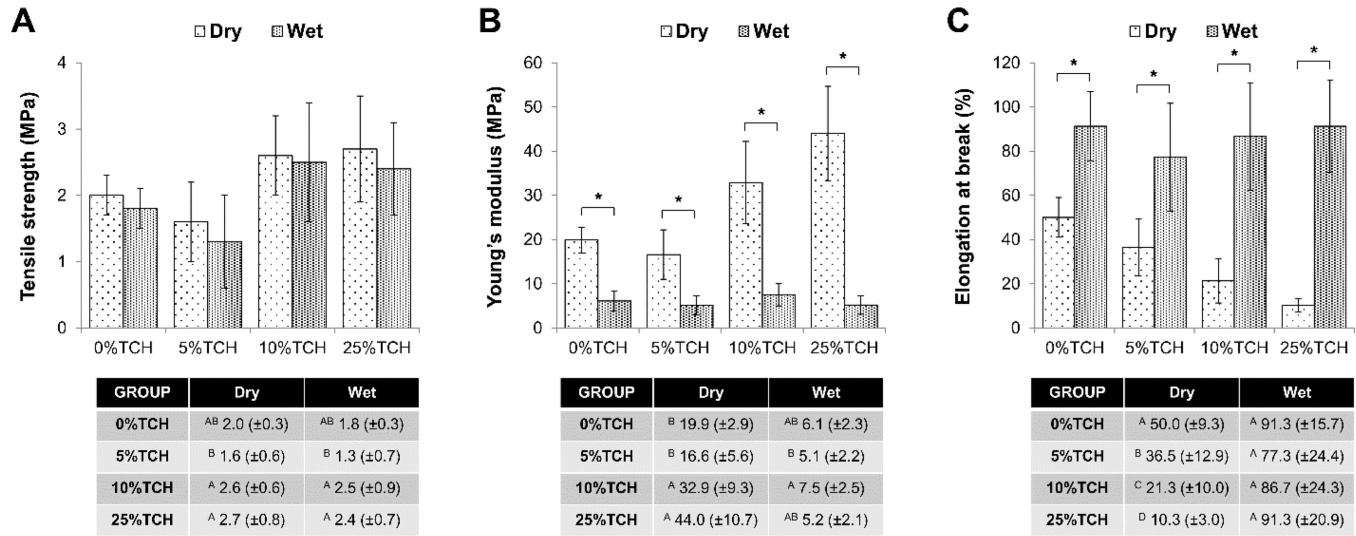
**Figure 1.**

(A) Representative SEM images of the distinct PLA:PCL/GEL-based fibers containing 0 (tetracycline-free), 5, 10, and 25% of TCH; Note the three-dimensional fibrous network with micron-sized porosity. (B) The fiber diameter distribution and mean fiber diameter ( $\pm SD$ ) (inset); Similar uppercase letters next to the ( $\pm SD$ ) indicate no significant differences at the P 0.05 level. (C) FTIR spectra confirming the incorporation of TCH into the electrospun PLA:PCL/GEL polymer-based fibers. Note the presence of characteristic peaks of TCH.

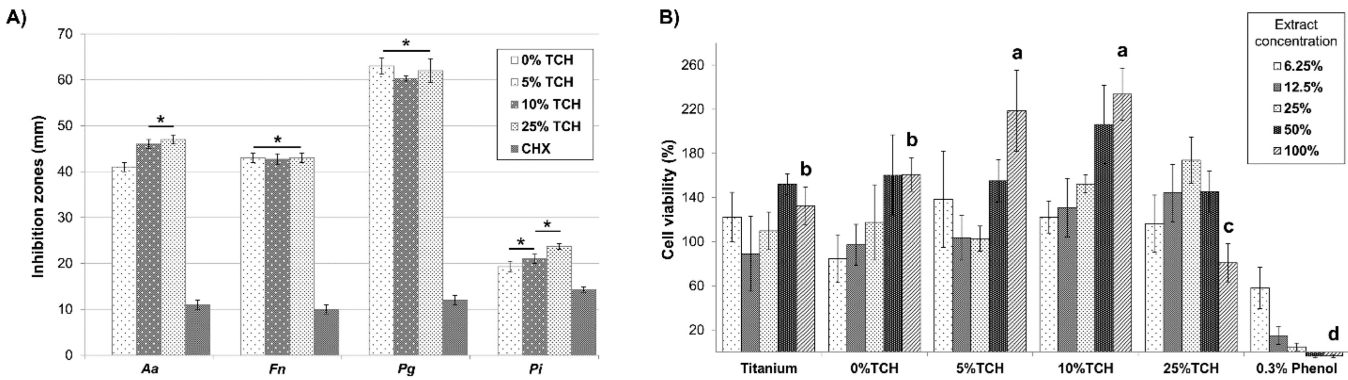


**Figure 2.**

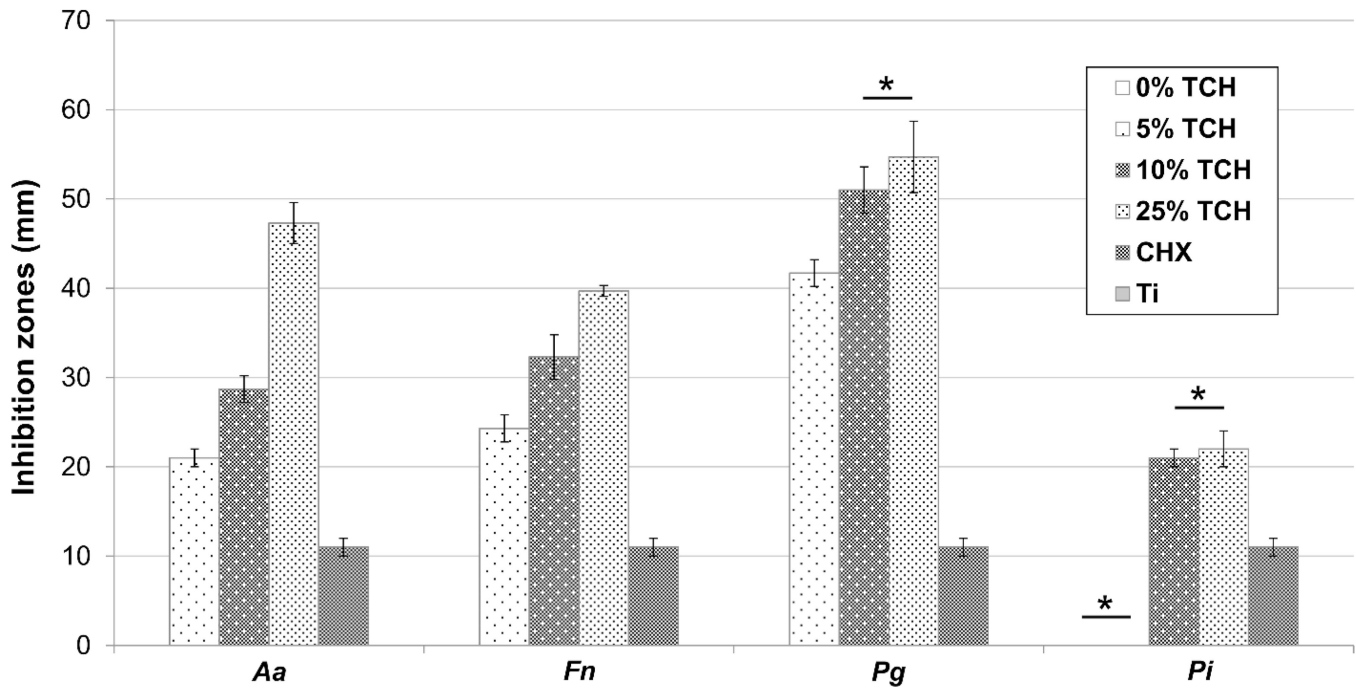
Drug release (%) profiles from electrospun polymer-based fibers incorporated with distinct amounts of tetracycline.

**Figure 3.**

Mechanical properties of the TCH-free and TCH-incorporated electrospun mats, under dry and hydrated testing conditions: (A) Tensile strength, in MPa; (B) Young's modulus, in MPa; and (C) Elongation at break, in %. Asterisks indicate a statistically significant difference exists between the two conditions (\* p < 0.05). Error bars indicate standard deviation of the mean.

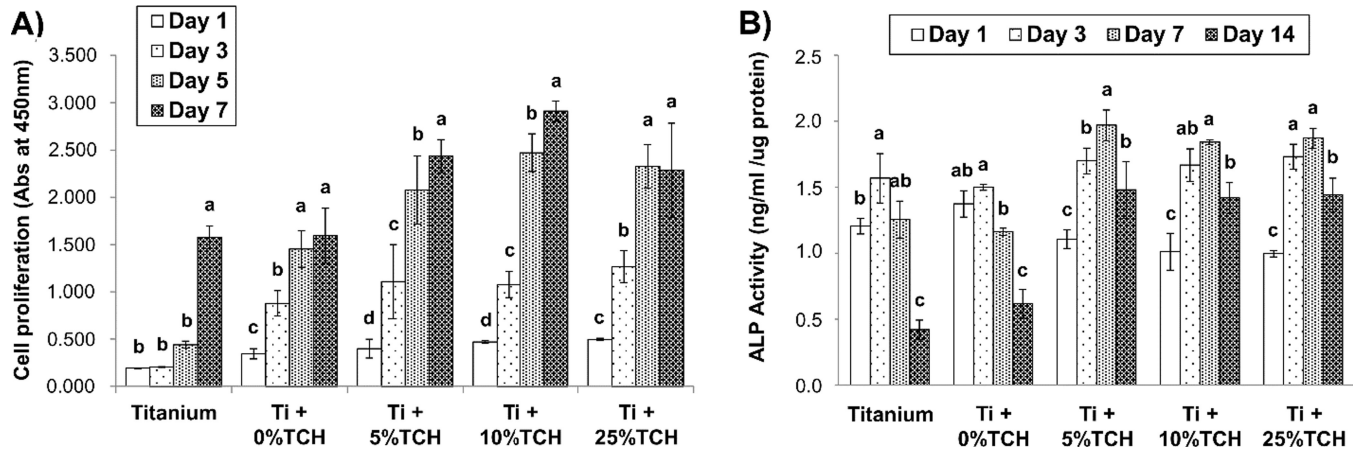
**Figure 4.**

Antimicrobial properties (inhibition zones, in mm) of the TCH-incorporated fibers against *Aa*, *Fn*, *Pg*, and *Pi*. The TCH-incorporated fibers were compared with a known antimicrobial solution (i.e., chlorhexidine gluconate at 0.12%, CHX). (B) Cytotoxicity assay data of the TCH-incorporated electrospun polymer fibers.

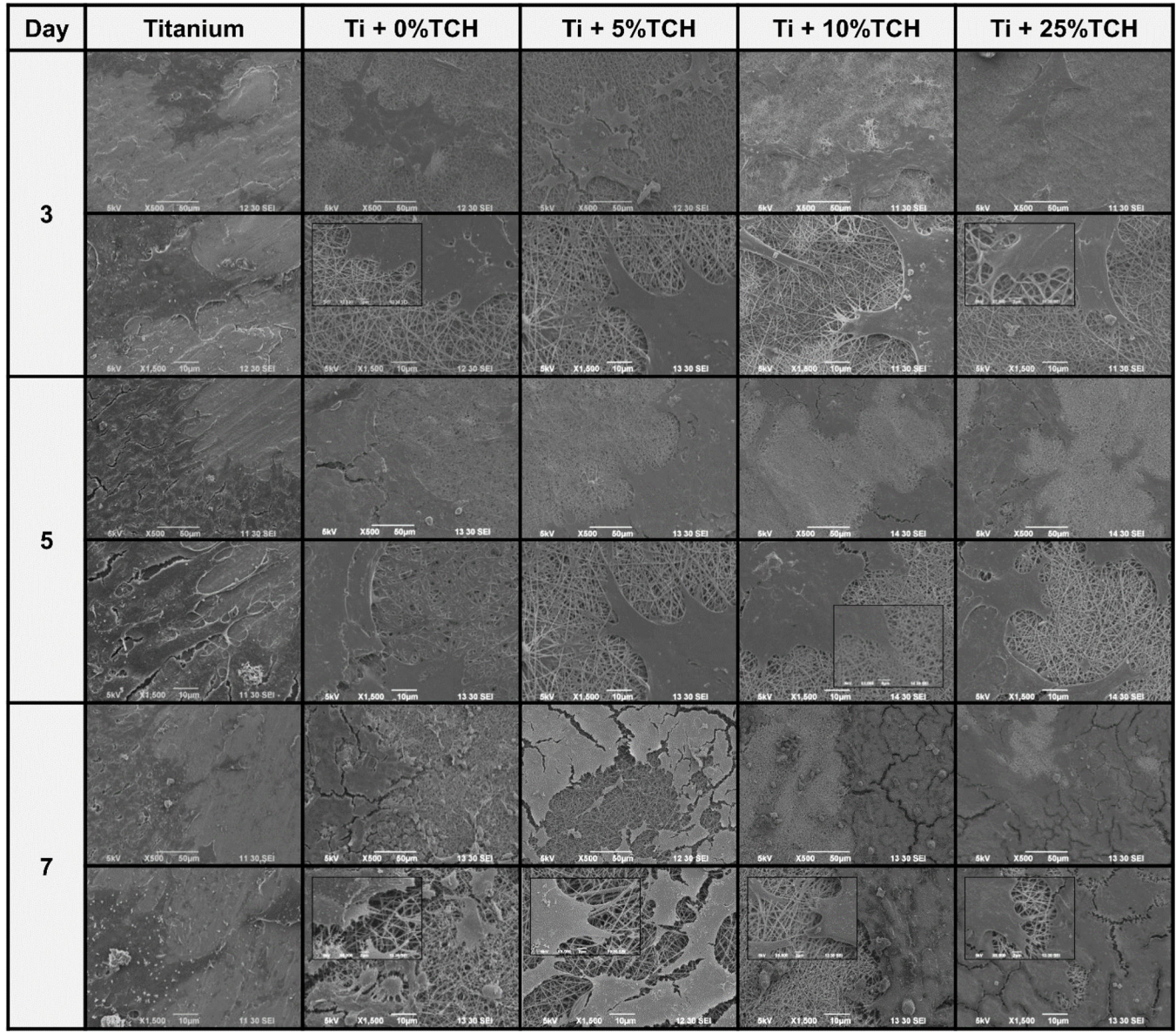


**Figure 5.**

Antimicrobial properties (inhibition zones, in mm) of the TCH-incorporated nanofiber-modified Ti disks against *Aa*, *Fn*, *Pg*, and *Pi*. The TCH-incorporated nanofiber-modified Ti disks were compared with CHX and bare (un-modified) Ti disks.

**Figure 6.**

(A) Cell proliferation (WST-1<sup>®</sup>) results of MC3T3-E1 on TCH-incorporated nanofiber-modified Ti disks after 1, 3, 5 and 7 days of cell seeding. (B) Normalized (the results were normalized to the total protein and expressed as ng of *p*-nitrophenol produced per mL per  $\mu$ g of protein) ALP activity of cell lysates from pre-osteoblasts (MC3T3-E1) after 1–14 days in culture. ALP activity was similar for all groups at days 1 and 3 but a significant increase in ALP levels on the Ti disks modified with TCH-incorporated nanofibers (5, 10, and 25 wt.%) was noticed on days 7 and 14. ALP activity decreased by day 14 in all the samples. There was no statistically significant difference in ALP levels among the TCH-incorporated fibers-modified Ti.

**Figure 7.**

Representative SEM images depicting cell proliferation of pre-osteoblasts within the nanofiber-modified Ti groups and bare Ti up to day 7.